ELSEVIER

Journal of Alloys and Compounds 330–332 (2002) 601–606

Journal of ALLOYS AND COMPOUNDS

www.elsevier.com/locate/jallcom

# Hydrogen absorption and desorption in mechanically alloyed titanium–chromium composites

J.F. Fernández*, C.R. Sánchez

*Dpto. Física de Materiales, Facultad de Ciencias, Universidad Autónoma de Madrid, Cantoblanco, 28049 Madrid, Spain*

**Abstract**

Ti and Cr composites with different compositions were prepared by mechanical alloying. Morphological, structural and compositional characterisation of the composites was accomplished by scanning electron microscopy, energy dispersive X-ray analysis and X-ray diffraction. The composites showed improved $H_2$ absorption and desorption kinetics compared to Ti. Improved kinetics is thought to be related to the formation, at the surface of the composite, of a Ti and Cr intermetallic compound with good activation properties. 

*Keywords:* Ti; Cr; Intermetallic compound; Composites; Hydrogen absorption/desorption; Mechanical alloying

## 1. Introduction

One of the main issues of metal–hydrogen systems research is the improvement of their activation characteristics. Metal hydrides activation comprises a number of steps aiming to obtain reproducible $P–C–T$ curves and hydrogen absorption/desorption kinetics. Activation procedures in practical applications represent a waste of money and for this reason, their shortening or elimination is a technical need. Another important issue in metal hydrides research is surface contamination taking place during cycling which results in a loss of hydrogen storage capacity and very poor hydrogen absorption/desorption kinetics, in consequence reducing significantly the operational life of the application.

A new idea has been developed recently to produce improved surface properties materials for hydrogen absorption and desorption. Although during the last decade several methods have been implemented [1–4], there is a basic idea common to all of them: the material is composed of two components, a majority component (active component) with good properties for hydrogen storage or battery applications (Mg alloys [1–3,5,6], $LaNi_5$ [2,7], $AB_2$ compounds [4,7], etc.) and a minority component (additive) with good surface properties for hydrogen absorption and desorption (Pd [2], intermetallic (IM) compounds [1,3–7], etc). In the case of metal–hydrogen systems, the word ‘composite’ is usually employed to designate this kind of material.

## 2. Experimental

The Ti–Cr composites were prepared by mechanical alloying (MA) using different weight percentages (wt. %) of Cr to Ti. In all cases, Ti was the active component and Cr and a Ti–Cr IM alloy ($TiCr_{1.85}$, C-15) were used as additives. The IM compound was prepared by arc melting. Ti sponge (99.5% purity and a particle size in the range 200 μm–1.5 mm) was mixed with either Cr (99.7%, 40 μm) or the $TiCr_{1.85}$ alloy (~20 μm particle size) in a stainless steel container (80 ml) with stainless steel balls of 10 mm in diameter and ~34 g mass. For all preparations, the ball-to-metal mass ratio was in the order of 3:1. The container was filled with argon and set in a planetary ball-mill machine (Fritsch ‘Pulverisette 6’). The composites were milled at an acceleration of 140 m $s^{-2}$ in a sequence of 1-min milling to 4-min pause. The sequence was repeated several times to complete a given total milling time. The main characteristics of the different composites prepared are given in Table 1. Two different milling times, 10 min and 70 min, were used.

Morphological, structural and compositional composite characterisation was performed before and after hydrogenation by means of X-ray diffraction (XRD), scanning

*Corresponding author.

*E-mail address:* josefrancisco.fernandez@uam.es (J.F. Fernández).

0925-8388/02/$ – see front matter 
PII: S0925-8388(01)01524-9

Table 1
Main characteristics of the composites

| Label | Type of additive | Total milling time (min) | Wt. % of Cr in ball-mill container | EDX results | |
|---|---|---|---|---|---|
| | | | | Wt. % of Cr (near surface region) | Wt. % of Cr (cross-section) |
| TiCr1 | Cr | 10 | 1.5 | 10 (1) | <0.3 |
| TiCr4 | Cr | 10 | 4.4 | 29 (7) | <0.3 |
| TiCr21 | Cr | 10 | 21.3 | 75 (3) | <0.3 |
| TiCr65 | Cr | 70 | 65.0 | 67 (5) | 68 (10) |
| TiTiCr1 | $TiCr_{1.85}$ (C-15) | 70 | 1.0 | 1.4 (0.3) | 1.1 (0.3) |
| TiTiCr6 | $TiCr_{1.85}$ (C-15) | 70 | 6.4 | 6.0 (0.8) | 6 (3) |
| Ti | – | 70 | – | – | – |
| $TiCr_{1.85}$ (C-15) | – | – | 67 (1)* | – | 65.3 (0.6) |

The Cr wt. % as mesured by EDX analysis is given in columns 5 and 6. *Nominal wt. % of Cr in the IM compound.

electron microscopy (SEM) and energy dispersive X-ray analysis (EDX). Diffraction patterns were acquired with Cu $K_\alpha$ radiation in a Siemens D-500 diffractometer. SEM images were obtained with a Phillips XL30 microscope equipped with EDX analysis (20 KeV).

After milling, about 0.7 g of the composite was introduced in a Sieverts type apparatus, described elsewhere [8], to study their hydrogen absorption and desorption properties. Hydrogen absorption was measured from the pressure drop in a calibrated volume at room temperature while hydrogen desorption was measured by thermal desorption technique. The sample temperature was accurately measured with a thermocouple in direct contact with the sample. Prior to $H_2$ absorption experiments, the samples were subject to an activation procedure consisting of one cycle of hydrogen absorption and desorption.

## 3. Results and discussion

### *3.1. Morphology, composition and structure of the composites*

No significant reduction in particle size was obtained with the milling conditions used in this work. Ti particles, with initially irregular shapes experience mainly plastic deformation during the milling operation. At the end of the process they have a flake-like shape where one dimension is much smaller than the other two. All composites prepared in this work showed a similar morphology.

EDX analyses were made on composite particles in as ball milled state and on polished particles. The wt. % of Cr to Ti is measured in a near surface region (~2 μm) in the first case and in the particle's cross section in the second one. Results are given in Table 1, columns 5 and 6. Numbers in parentheses give standard deviation of several measurements in different particles. The accuracy of EDX measurements was checked using a well known Ti and Cr composition IM compound ($TiCr_{1.85}$, 67 wt. % Cr) and EDX measurement results are given in the last row of Table 1. From these measurements, the EDX results can be considered reliable. Once hydrogenated, the composites show values for the wt. % of Cr similar to those quoted in Table 1. It should be pointed out that very little iron contamination was detected in the EDX analysis at the conditions used in the ball-milling operation.

Fig. 1 shows the overlapped X-ray maps of Ti and Cr (sum X-ray map) for TiCr1 (a) and TiCr21 (b) composites at the near surface region together with their corresponding SEM images (c, d). Both images correspond to an area of ~100×100 $\mu m^2$. The X-ray maps show different zones clearly, the brighter ones correspond to Cr-rich areas while the darker ones correspond to Ti-rich areas.

Structural data from XRD patterns show that the additive is incorporated in its elemental form and no signs of any phases other than those of the parent components, i.e. Ti-hcp and either Cr-bcc or $TiCr_{1.85}$-C15, are observed within the detection level of this technique (~1–2% under the conditions of our measurements).

For shorter milling times (Table 1, rows 1–3), the wt. % of Cr at the near surface region (column 5) is always higher than the amount added to the ball-mill container (column 4). In addition, no Cr is observed in cross-sectional measurements (column 6). So, at this shorter milling time, Cr is mainly incorporated to the surface. By increasing the Cr content in the ball-mill container, an increment in the Cr coverage of the Ti particles is produced (see Table 1 and Fig. 1a and b).

A different picture is obtained for samples milled for a longer time (rows 4–6). In these cases the wt. % of Cr measured by EDX at the near surface region and that obtained from cross-sectional measurements (columns 5 and 6) are similar and comparable to the amount of Cr added (column 4). This seems to suggest that, besides Cr incorporation to the Ti surface, continuous cold welding and fracture become important factors at this longer milling time. The net effect is an almost homogeneous distribution of Cr in the Ti bulk.

### *3.2. Hydrogen absorption/desorption properties of the composites*

Absorption properties of the composites were studied at room temperature after the activation treatment (see Sec-

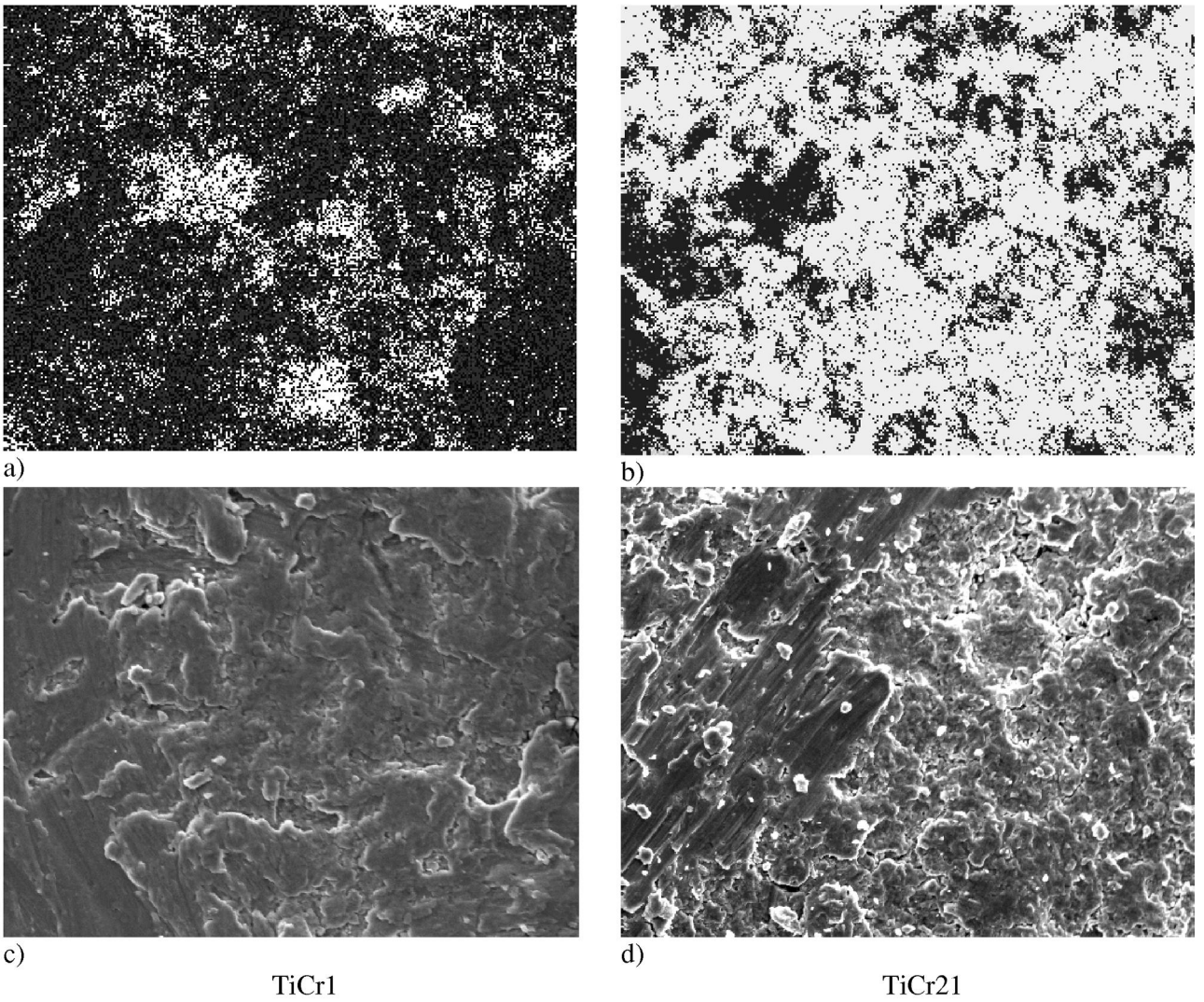


Fig. 1. X-Ray map-sum for Ti and Cr and corresponding SEM inages of the composites TiCr1 (a, c) and TiCr21 (b, d).

tion 2). In some of the experiments the samples were fully hydrogenated by introducing a single allotment of hydrogen to the system whereas, in other cases, it was achieved in several steps. The hydrogen absorption results of Fig. 2a–c correspond to samples hydrogenated in three steps. In that figure, the reacted fraction increment with time for composites TiCr1, TiCr4 and TiCr21 and for a titanium sample (no additive) is shown. The reacted fraction represents the active sample fraction that becomes fully hydrogenated.

In order to compare absorption properties of different composites it is important that the sample temperature remains constant during the absorption process. In the hydrogen absorption experiments shown in Fig. 2a–c, temperature increment was negligible for the first allotment (a), about 5°C for the second one (b) and varied from negligible values to 120°C (in the case of the TiCr21 composite) for the last one (c). In the last case, the sample temperature came back to room temperature after about 30 min and then most of the data shown in Fig. 2c are obtained with the sample at room temperature.

On the other hand, the H-absorption rate for TiCr65 composites was so high that it was impossible to keep the sample temperature close to room temperature (temperature increased up to 500°C), the full hydrogenation process taking place in a few minutes, but at high temperature. Although this precludes direct comparison with the results of Fig. 2, it indicates that hydrogen is absorbed quite fast in those composites.

Results presented in Fig. 2 show that the addition of Cr to Ti improves hydrogen absorption kinetics. The effect is clear for the first and second $H_2$ gas allotment (Fig. 2a and b) but it is not so clear for the last allotment when full hydrogenation is achieved. In this case, apart from some differences at the beginning of the absorption process, the curve slopes at times longer than 200 min are almost identical, independently of Cr content. This can be understood by considering the Ti hydrogenation process [9,10].

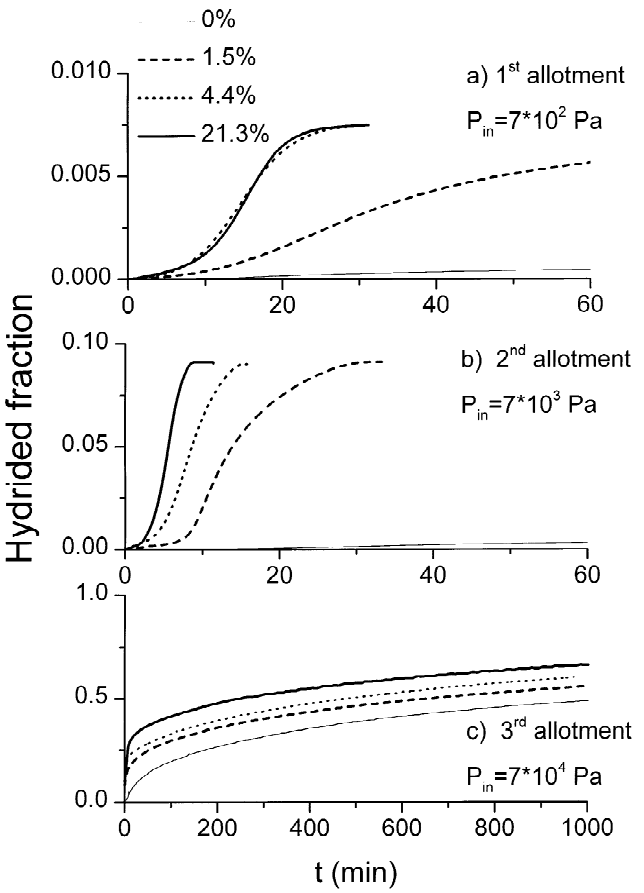


Fig. 2. Absorption curves at room temperature for samples Ti, TiCr1, TiCr4 and TiCr21. The initial applied pressure for each allotment is given in the legend.

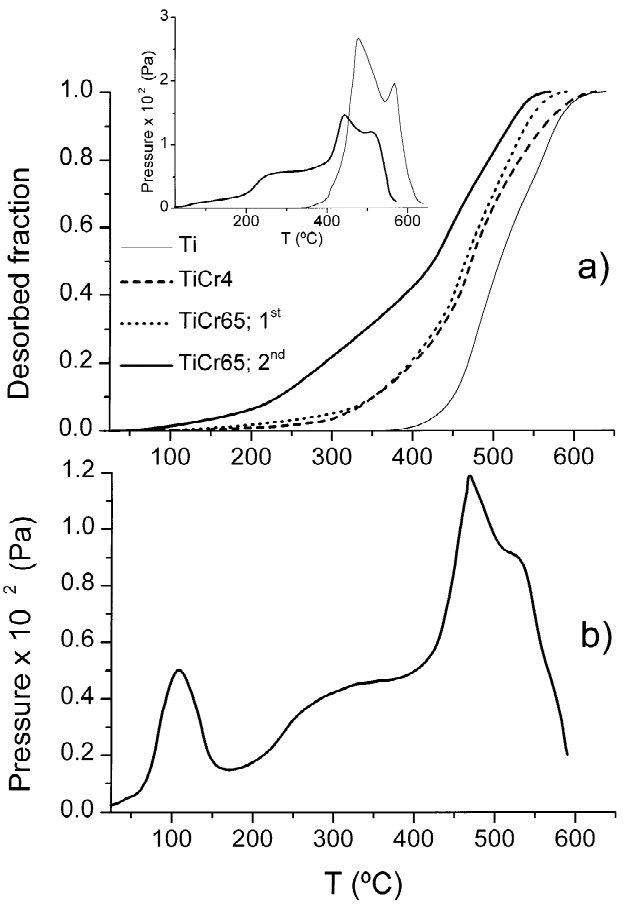


Fig. 3. (a) Desorbed fraction as a function of temperature for several composites (see legend in figure). The inset compares TD spectra for a virgin Ti and for a TiCr65 composite. (b) TD spectra of TiCr65 sample subject to several $H_2$ absorption/desorption cycles.

Because of the very low $H_2$ equilibrium pressure of Ti at room temperature, a surface hydride layer of high hydrogen content ($x$~2) is formed at the beginning of the hydrogenation process. Eventually, this hydride layer progresses from the surface to the bulk until hydrogenation of the whole particle. Fig. 2a and b correspond to the first part of the hydrogenation process when the surface hydride is developing. On the other hand, the increment of reacted fraction shown in Fig. 2c reflects how the surface hydride layer progresses in depth. This is controlled by the diffusion of hydrogen in the titanium bulk which should not be affected by the added Cr.

It should be expected that the hydrogen desorption kinetics of the composites are also dependent on their Cr content. This study was done by thermal desorption (TD) experiments in the fully hydrogenated composites. Fig. 3a shows the desorbed fraction as a function of temperature for a virgin Ti sample (thin solid line) and for the composites TiCr4 (dashed line) and TiCr65 (one and two $H_2$ absorption/desorption cycles, dotted and thick solid lines, respectively). The TD spectra for TiCr1 and TiCr21 were similar to that of TiCr4. The inset in Fig. 3a compares the pressure evolution with temperature for the Ti and for the second desorption run of the TiCr65 sample. In Fig. 3b, the TD spectra of another TiCr65 composite after several absorption/desorption cycles is depicted. This data will be used later.

It is clear from Fig. 3a, that Cr addition improves $H_2$ desorption kinetics. This is seen by a reduction on the onset temperature for desorption which is almost room temperature for TiCr65 (second run) and ~150°C for TiCr4 and TiCr65 (first run) compared to 350°C in the virgin Ti. What is the reason for such improvement?

Passivation of the Ti surface by impurities produces mainly a reduction in the sticking coefficient of hydrogen [9]. If Cr is able to improve the Ti absorption/desorption properties it should be either because it reduces the Ti surface contamination or because it increases the sticking coefficient of hydrogen. One possibility is the formation on the surface of the composite, of a Ti–Cr IM compound with good activation characteristics. In fact, potential IM compounds exist and correspond to any of the Laves phases, C-15, C-14, that Ti and Cr form at about 65 wt. % Cr. These IM compounds absorb hydrogen at room temperature at a very fast rate but they are too unstable for

practical applications [11]. We believe that this mechanism is responsible for the improved kinetics of the composites. Two pieces of information supporting that idea are given below.

Fig. 4 shows XRD patterns from the as prepared TiCr65 (dashed) and the partially hydrogenated TiCr65 (solid) and TiCr21 (dotted) composites. The TiCr65 composite was subjected to several absorption/desorption cycles while TiCr21 was subjected to only one cycle. The XRD patterns show the Ti-hcp, $TiH_2$-fcc and Cr-bcc phases expected but also, for the hydrogenated TiCr65, the most intense lines of the $TiCr_{1.85}H_x$ C-15 Laves phase can be observed. It is possible that this phase is also present in the TiCr21 composite but the signal is to low to be conclusive. As mentioned before, the XRD patterns of the composites before being exposed to hydrogen do not show any sign of alloy formation and this can be seen from Fig. 4 (dashed curve). That means that the $TiCr_{1.85}H_x$ C-15 phase is formed in the hydrogen absorption/desorption process.

A second piece of information comes from TD results for the TiCr65 composite (Fig. 3b) whose XRD data have been shown above. The main difference with the other curves in the inset of Fig. 3a is the desorption peak at about 100°C. The desorption of hydrogen from titanium has been studied in detail by Malinowski in a series of papers [12,13] and from those results, we can conclude that the peak observed in Fig. 3b at low temperature cannot be due to desorption from Ti. Taking into account the high instability of any of the Ti–Cr IM compounds, which anticipates hydrogen desorption at very low temperatures, and considering XRD patterns presented in Fig. 4, it seems reasonable to assign the 100°C peak to hydrogen desorption from this IM compound.

## 4. Conclusions

Cr incorporation into Ti particles has been achieved in a highly efficient way by mechanical alloying. At low milling times, Cr is incorporated mainly into the Ti particle surface. By increasing the milling time, continuous cold welding and fracture becomes important and an homogeneous distribution of Cr in the Ti is produced.

The composites show improved hydrogen absorption and desorption kinetics compared with that of virgin Ti at room temperature. The likely mechanism responsible for such improvement relies on the formation in the Ti particle surface of a Ti–Cr IM compound with very good activation properties. This compound is formed during the hydrogen absorption/desorption cycles. In this compound

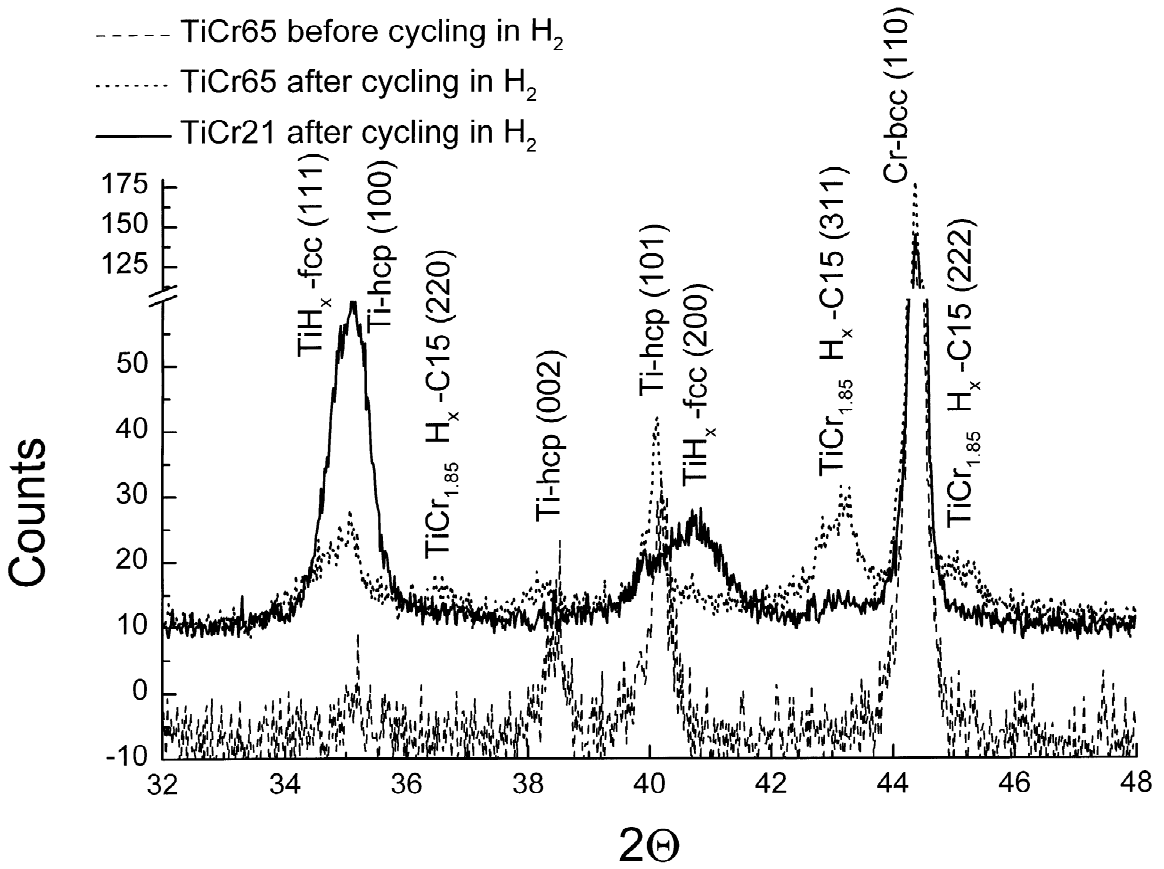


Fig. 4. X-Ray diffraction patterns of the as-prepared TiCr65 composite (dashed curve) and the partially hydrogenated TiCr21 and TiCr65 composites (solid and dotted curves, respectively). The different phases are indicated in the figure.

hydrogen molecules split into atoms that diffuse across the IM compound to Ti bulk.

## Acknowledgements

This work has been supported by DGICYT (PB96-0084) and CAM (07N/0008/1999). Technical assistance by Fernando Moreno is greatly recognised.

## References

[1] P. Mandal, K. Dutta, K. Ramakrishna, K. Sapru, O.N. Srivastava, J. Alloys Comp. 184 (1992) 1–9.
[2] L. Zaluski, A. Zaluska, P. Tessier, J.O. Strom-Olsen, R. Schulz, J. Alloys Comp. 217 (1995) 295–300.
[3] K.J. Gross, P. Spatz, A. Zuttel, L. Schlapbach, J. Alloys Comp. 240 (1996) 206.
[4] E. Akiba, H. Iba, Intermetallics 6 (1998) 461–470.
[5] K.J. Gross, D. Chartouni, E. Leroy, A. Zuttel, L. Schlapbach, J. Alloys Comp. 269 (1998) 259.
[6] G. Liang, S. Boily, J. Huot, A. Van Neste, R. Schulz, J. Alloys Comp. 268 (1998) 302.
[7] Q. M Yang, M. Ciureanu, D.H. Ryan, J.O. Strom-Olsen, J. Alloys Comp. 274 (1998) 266.
[8] J.F. Fernández, F. Cuevas, M. Alguero, C. Sánchez, J. Alloys Comp. 231 (1995) 78–84.
[9] B. Kasemo, E. Tornquist, Appl. Surf. Sci. 3 (1979) 307–328.
[10] A. Efron, Y. Lifshitz, I. Lewkowicz, M.H. Mintz, J. Less-Common Met. 153 (1989) 23–34.
[11] J.R. Johnson, J.J. Reilly, Inorg. Chem. 17 (1978) 3103.
[12] M.E. Malinowski, J. Nucl. Mater. 85&86 (1979) 957–962.
[13] M.E. Malinowski, J. Less-Common Met. 89 (1983) 27–35.